



Research Article

TEMPERATURE EVALUATION AND BONDING QUALITY OF LARGE SCALE ADDITIVE MANUFACTURING THIN WALL PARTS

Ömer EYERCİOĞLU\*<sup>1</sup>, Mehmet ALADAĞ<sup>2</sup>, Samet SEVER<sup>3</sup>

<sup>1</sup>Mechanical Engineering Department, Gaziantep University, GAZIANTEP; ORCID:0000-0002-9076-0972

<sup>2</sup>Mechanical Engineering Department, Gaziantep University, GAZIANTEP; ORCID:0000-0002-2484-7519

<sup>3</sup>Mechanical Engineering Department, Gaziantep University, GAZIANTEP; ORCID:0000-0002-7418-6659

Received: 23.04.2018 Revised: 21.06.2018 Accepted: 09.07.2018

ABSTRACT

In this study, thermal evaluation of ABS polymer thin wall part fabricated by large scale additive manufacturing is presented. The cooling of single bead layers, the interface temperature and the effect of adjacent top layer on the temperature of the previous layer were investigated. The experimentally measured temperatures were compared one dimensional heat transfer model of a single filament. The measured temperature values are in general agreement with the model until the adjacent top layer is going to be deposited. While the interface temperature was below the glass transition temperature at the beginning of the process, it was gradually increased with additional layers. The tension tests carried out using the specimens which were cut parallel and perpendicular to the building directions, showed mechanical anisotropy of the printed sample. The interlayer strength is about the half of the longitudinal strength of the printed sample, although interface temperature between adjacent layers was above the glass transition temperature and subsequent rolling was performed.

**Keywords:** Additive manufacturing, direct extrusion, ABS, large scale, thermal imaging.

1. INTRODUCTION

Additive manufacturing methods have been mostly used for rapid prototyping, where these methods extensively used to assess the geometric and aesthetics aspects of designs [1]. In recent years, the use of additive manufacturing for functional products with required mechanical properties has increased significantly. In most of the commercially available 3D printing systems, the deposition rates and the building volumes are limited as 0.01-0.085 kg/h and 0.03-0.3 m<sup>3</sup>, respectively [2]. Therefore, they are not or less suited for larger parts. Large Scale Additive Manufacturing (LSAM) defines a system that can be used for printing components on the order of several meters at high extrusion rates (up to 50 kg/h). The feed stock material is in the form of thermoplastic or fiber reinforced thermoplastic pellets which are almost 20 times cheaper than the filament based feedstock. The system has the potential to significantly affect automobile, aerospace and energy industries.

For direct manufacturing of actual parts by using LSAM, both process parameters and feedstock material need improvements to meet the mechanical requirements. One of the biggest

\* Corresponding Author: e-mail: eyercioglu@gantep.edu.tr, tel: (342) 317 15 93

drawbacks of the LSAM process for functional use of components is mechanical anisotropy [2-6]. The components printed by LSAM, have lower strength in the building direction (across successive layers) than the in plane directions.

The temperature history of the extruded deposit is a critical parameter in dictating the part strength [5]. Therefore several heat transfer models have been proposed [7-10], thermal image measurements [11-13] and numerical analyses [1, 14] have been carried out in the previous works. Most of them are related to Fused Deposition Modeling (FDM) of relatively small parts. The thermal effect is more dominated in large scale additive manufacturing due to higher volume of material deposition. Yardımcı and Gucerı [7] developed a family of numerical models for fused ceramic deposition. Rodriguez-Matas [9] performed a transient 2D analysis of the FDM process by assuming the filament cross-section as rectangular. Li, *et al.* [10] used the lumped capacity analysis for modeling the cooling process of a single filament. They have used one dimensional transient heat transfer model and elliptical cross-section of the deposited filament. Costa *et al.* [12] presented an analytical solution to the transient heat conduction developing during FDM, which activates or deactivates all relevant local boundary conditions depending on part geometry, operating conditions and deposition strategy. Compton *et al.* [13] measured the thermal evolution of carbon fiber/ABS composite fabricated via BAAM and developed a one dimensional transient heat transfer model.

In this study the thermal evaluation of ABS thin wall part during large scale manufacturing was measured using infrared imaging. The test components are printed by using LSAM system which has developed in The Gaziantep University Mechanical Engineering Department CAD/CAM Laboratory. The cooling of single bead layers, the interface temperature and the effect of adjacent top layer on the temperature of the previous layer were investigated. The results were compared with the lumped capacity analysis of Li *et al.* [10]. The tension tests carried out using the specimens to mechanical anisotropy of the printed sample.

## 2. EXPERIMENTAL STUDY

### 2.1. Material

An Acrylonitrile Butadiene Styrene (ABS) thermoplastic polymer, with the properties shown in Table 1, was used in the experimental study. The granules were dried at 80 °C for 4 hours before using. The material is deposited at 210 °C onto heated building plate at 65 °C.

### 2.2. Printing System

A direct extrusion system shown in Figure 1 is designed, manufactured and it was replaced with the spindle of the 3-axes CNC unit available in the department. The maximum displacements in X Y and Z directions are 1800, 2500 and 400 mm, respectively. The extruder is a single screw extruder and it is driven by a variable speed motor. The ABS granules are feeding through the extruder by an automatic feeder. The amount of granules and the speed of screw can be controlled to melt and deposit molten polymer at a rate consistent with the movement of the axes (building speed) and desired bead profile. The barrel has band heaters and a control unit to keep the chamber and nozzle temperatures in the required ranges. In the experimental study 6 mm diameter nozzle was used. A rolling unit is also integrated to the system to spreading the wall width and bead profile.

**Table 1.** Material Properties of ABS

Property	Value
Density $\rho$ (kg/m <sup>3</sup> )	1060
Thermal conductivity $k$ (W/m K)	0.177
Specific heat $C$ (J/kg K)	2080
Emissivity $\epsilon$	0,87
Glass Transition Temperature $T_g$ (°C)	105

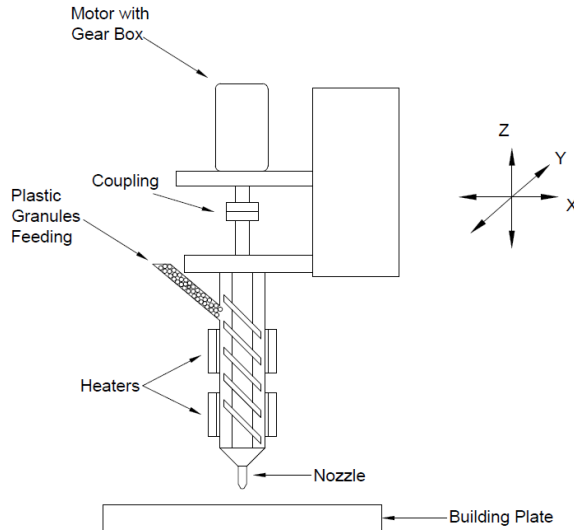


**Figure 1.** Schematic view of the direct extrusion system.

### 2.3. Experimental Procedure

Thin wall test components were printed on the system described above. The molten ABS exits the extruder (the 6 mm diameter orifice) and by the action of roller forms an oval bead with height of 3.5 mm and width of 15 mm. Single bead layers were printed by reciprocating (+X and -X directions) motion of the extruder head with a speed of 250 mm/min (see Figure 2). The temperature at the orifice exit is approximately 210°C. The first layer is deposited on an ABS sheet covered aluminum table (build plate) which is heated to 65°C. The temperature of the build plate kept constant during printing. A thermal camera (Testo 875-2i) was used for thermal images of the process and the captured frames were analyzed using Tesco IRSofT. The printing conditions are presented in Table 2.

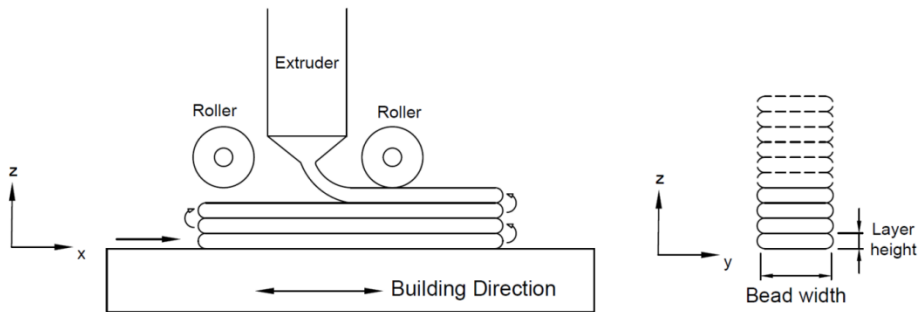


**Figure 2.** Building strategy and bead geometry

**Table 2.** Processing parameters

Parameter	Value
Extrusion temperature (°C)	210
Building plate temperature (°C)	65
Deposition rate (kg/h)	0.72
Nozzle diameter (mm)	6
Building speed (m/min)	0.25
Bead width (mm)	15
Bead height (mm)	3.5

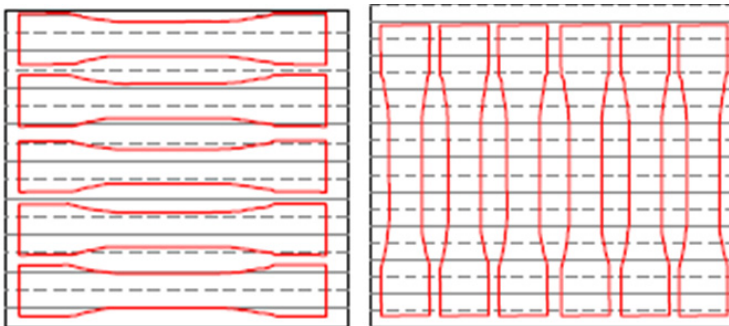


**Figure 3.** Orientation of tensile specimens

Tension tests (ASTM D638) were carried out to compare the mechanical anisotropy of the printed samples. The specimens were cut parallel and perpendicular to the building directions by using CNC milling machine as shown in Figure 3. The dimensions of the specimens are given in figure 4. A 10 kN capacity Shimadzu AGS-X tensile testing machine was used for the tests.

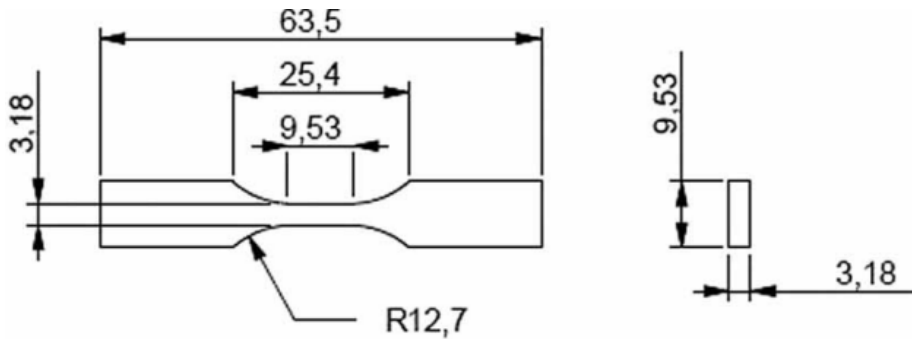


Figure 4. Dimensions of tensile specimens according to ASTM D638

### 3. RESULTS AND DISCUSSION

#### 3.1. Thermal Analysis

The bonding ability and strength of the printed part is depending on the thermal history of the deposited bead. The temperature time history of the first layer (L1) which is deposited on the building plate (pre-heated to 65°C) is shown in Figure 5 for 15 mm thick wall with a 60 seconds extrusion time, printed using 6 mm diameter orifice. The measurement is taken from the mid-section of the printed bead (half length). The temperature of the molten deposit is approximately 209°C at the exit of the nozzle and gradually decreases to 90°C in 60 seconds where the extruder head moves 250 mm (completes one layer and turn back to mid-section while printing second layer). The temperature of second layer heats up the existing layer approximately 140°C in seconds.

This result can be compared with the lumped capacity analysis of Li *et al.* [10] for modeling the cooling process of the extruded filament. In the analysis, one dimensional heat transfer model of a single filament was used and the cross-sectional shape of the deposited filament was modeled as an ellipse. The analytical solution proposed by Li *et al.* [10] is as follows:

$$T = T_E + (T_L - T_E)e^{-mx} \tag{1}$$

The terms T, T<sub>E</sub> and T<sub>L</sub> are bead temperature at any time (t), envelope temperature and orifice temperature, respectively. With:

$$m = \frac{\sqrt{1+4\alpha\beta}-1}{2\alpha} \text{ and } x = vt \tag{2}$$

where:

$$\alpha = \frac{k}{\rho Cv} \quad \text{and} \quad \beta = \frac{hP}{\rho CA v} \tag{3}$$

The symbols A, P and v represent the cross-sectional area of the bead, the perimeter of the bead and its deposition speed, respectively. The continuous line in Figure 5 shows the results calculated by using equations 1-3 with input data given in Table1 and Table 2.

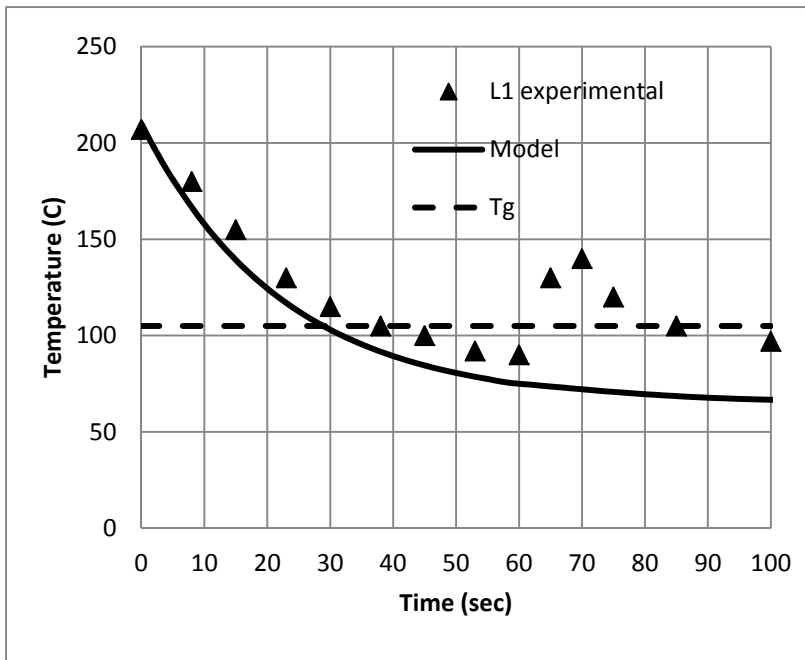


**Figure 5.** The cooling of the first layer (L1)

The measured data are in general agreement with the model as shown in Figure 5. The experimental results obtained from thermal images have similar trend with the model in spite of a little higher values. The temperature of the molten deposit reaches to glass transition temperature ( $T_g$ ) about 30 seconds. Due to the time required to complete a layer is 60 seconds (part length is 250 mm and the speed of head is 250 mm/min), the interface temperature ( $90^{\circ}\text{C}$ ) is lower than the glass transition temperature for the first layer. The thermal images of the process and the captured frames at 305, 480 and 540 seconds are given in Figure 6. Figure 7 shows the time evolution of the temperature of the extruded deposit 1-10 layers at the mid-section. As a new layer is deposited, the temperature of the adjacent layers increases so their cooling is delayed. Each peak was followed by rapid decrease in temperature as the extrusion head moved away from the center position of the part. The temperature of the mid-section was gradually increasing during process and the interface temperature was higher than the glass transition temperature after third layer (L3). This shows that cooling may be required during process to keep the shape of the bead. For longer parts, deposition times between layers are longer; more cooling of the interface reduces surface temperature below the glass transition, therefore heating the surface may require [2].

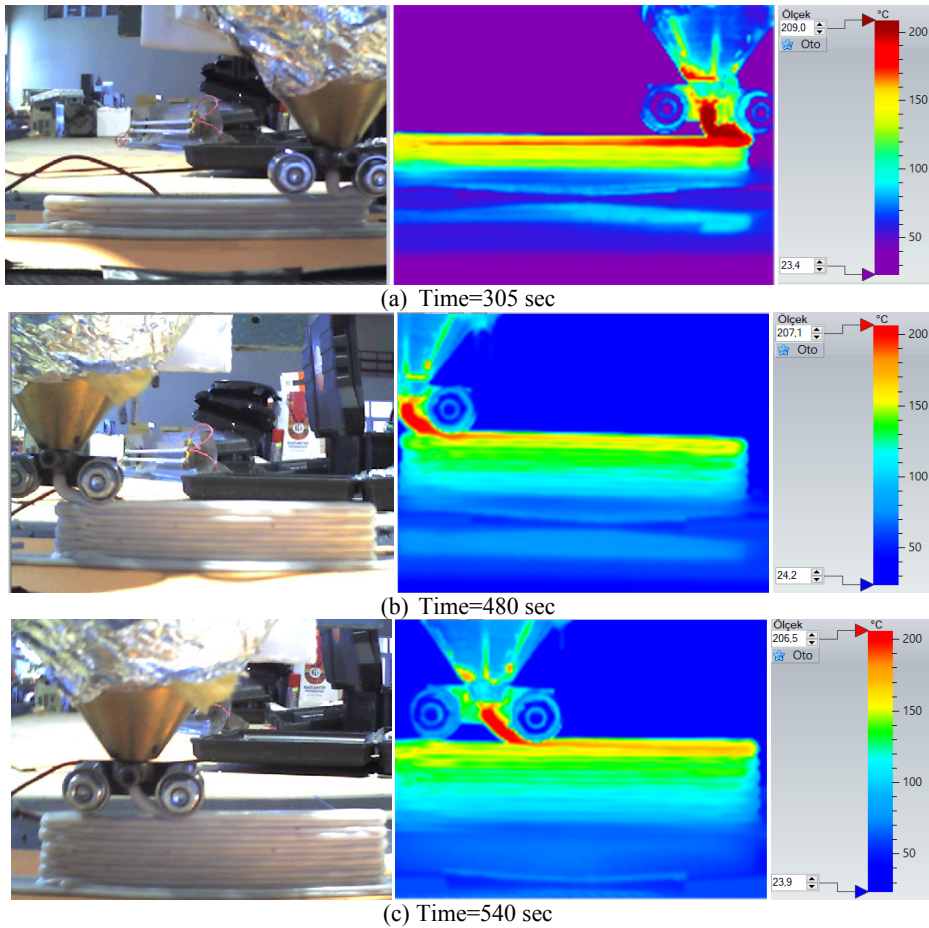


**Figure 6.** Thermal images of the process at a) 305 seconds b) 480 seconds c) 540 seconds

### 3.2. Tension Tests

The stress-strain diagram obtained from the tension tests is shown in Figure 8. The mechanical anisotropy of the printed sample is very clear. The ultimate strengths of the specimens were cut parallel and perpendicular to the building directions are about 22.3 MPa and 10.6 MPa, respectively. From the extensometer readings Shimadzu Trapezium X Universal Testing Software reports that the Young's Moduli values are about 2.3 GPa and 1.9 GPa, respectively. Although, interface temperature between adjacent layers was above the glass transition temperature and subsequent rolling was performed, the interlayer strength is about the half of the longitudinal strength. Keeping in mind that the specimens were as printed condition and no post-curing was applied. The sintering phenomenon was found to have significant effect on bond formation as indicated previously [4].

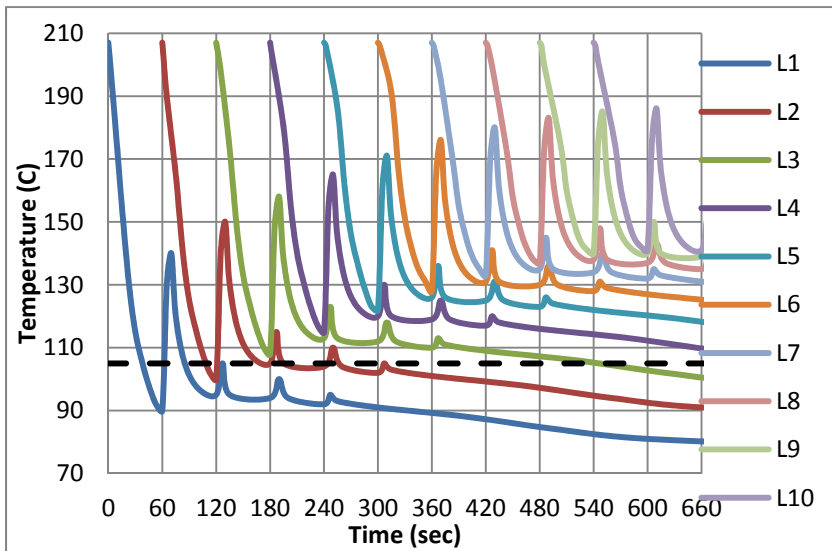


**Figure 7.** The time evolution of the temperature of the extruded deposit 1-10 layers at the mid-section.

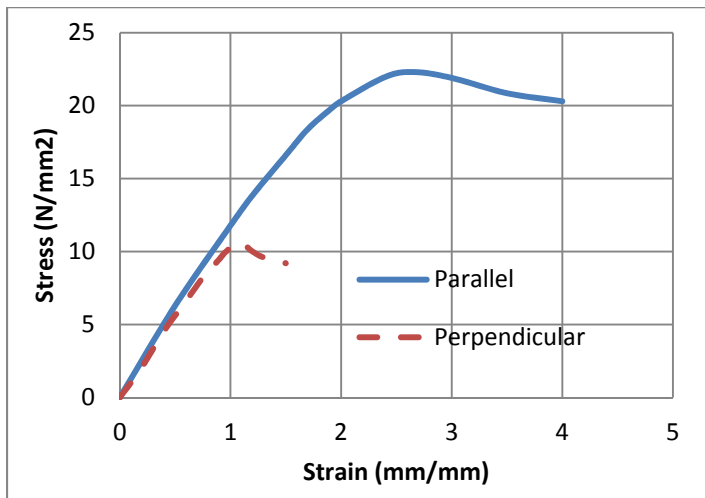


**Figure 8.** Tension test results of the specimens were cut parallel and perpendicular to the building directions

#### 4. CONCLUSIONS

In this study the thermal evaluation of ABS thin wall part during large scale manufacturing was measured using infrared imaging. The cooling behavior of the first layer was compared with the lumped capacity analysis of Li *et al.* [10] in which one dimensional heat transfer model of a single filament was used. The measured data are in general agreement with the model until the

adjacent top layer is going to be deposited. As a new layer is deposited, the temperature of the adjacent layers increases. The heat of the new layer causes a peak followed by rapid decrease in temperature as the extrusion head moved away from the center position of the part. The temperature of the mid-section was gradually increasing during process and the interface temperature was higher than the glass transition temperature after third layer (L3). This shows that cooling may be required during process to keep the shape of the bead. For longer parts, deposition times between layers are longer; more cooling of the interface reduces surface temperature below the glass transition, therefore heating the surface may require [2].

The tension tests carried out using the specimens were cut parallel and perpendicular to the building directions showed mechanical anisotropy of the printed sample. The interlayer strength is about the half of the longitudinal strength of the printed sample, although interface temperature between adjacent layers was above the glass transition temperature and subsequent rolling was performed. The specimens were not sintered before the tests to show the properties of the part as printed condition. This shows the necessity of sintering process to increase bonding properties. Further investigation on the bonding quality in terms of part size and rolling parameters are needed.

## REFERENCES

- [1] Talagani, M. R., DorMohammadi, S., Dutton, R, *et al.* Numerical Simulation of Big Area Additive Manufacturing (3D Printing) of a Full Size Car, SAMPE Journal, v. 51, no. 4, July/August, pp. 27-36, 2015.
- [2] Kishore, V., Ajinjeru, C., Nycz, A., Post, B., Lindahl, J., Kunc, V., Duty, C., Infrared Preheating to Improve Interlayer Strength of Big Area Additive Manufacturing (BAAM) Components, Additive Manufacturing, 14, pp. 7-12, 2017.
- [3] Duty, C. E., Kunc, V., Compton, B. G., Post, B. K. *et al.* Structure and Mechanical Behavior of Big Area Additive Manufacturing (BAAM) Materials, Rapid Prototyping J., 23, 1, pp. 181-189, 2017.
- [4] Faes, M., Ferraris, E., Moens, D., Influence of Inter-layer Cooling Time on the Quasi-static Properties of ABS Components Produced via Fused Deposition Modelling, Procedia CIRP, 42, pp. 748-753, 2016.
- [5] Sun, Q., Rizvi, G. M., Bellehumeur, C. T., Gu, P., Effect of Processing Conditions on The Bonding Quality FDM polymer Filaments, Rapid Prototyping J., v. 14, n 2, pp. 172-80, 2017.
- [6] Sung, H. A., Montero, M., Odell, D., Roundy, S., Wright, P. K., Anisotropic Material Properties of Fused Deposition Modeling ABS, Rapid Prototyping J., v. 8, n 4, pp. 248-257, 2002.
- [7] Yardımcı, M. A., Güceri, S., Conceptual Framework for the Thermal Process Modeling of Fused Deposition, Rapid Prototyping J., v. 2, n 2, pp. 26-31, 1996.
- [8] Rodriguez-Matas, J. F. Modeling the Mechanical Behavior of Fused Deposition ABS Polymer Components, PhD Dissertation, department of Aerospace and Mechanical Engineering , Notre Dame, IN., 1999.
- [9] Thomas, J. P., Rodriguez, J. F. Modeling the Fracture Strength Between Fused deposition extruded Rods, Solid Freeform Fabrication Symposium Proceedings, Austin, TX, USA, 2000.
- [10] Li, L., Gu, P., Sun, Q., Bellehumeur, C., Modeling of Bond Formation in FDM Process, The Transactions of NAMRI/SME, v31, pp. 613-620, 2003.
- [11] Shaffer, S. Yang, K., Vargas, J., Di Prima, M., Voit, W., On Reducing Anisotropy in 3D Printed polymers via Ionizing Radiation, Polymers, 55, pp. 5669-5679, 2014.

- [12] Costa, S. F., Duarte, F. M., Covas, J. A., Estimation of Filament Temperature and Adhesion Development in Fused Deposition Techniques, *J of Materials Processing Technology*, 245, pp. 167-179, 2017.
- [13] Compton, B. G., Post, B. K., Duty, C. E., Love, L., Kunc, V., Thermal Analysis of Additive Manufacturing of Large Scale Thermoplastic Polymer Composites, *Additive Manufacturing*, 17, pp. 77-86, 2017.
- [14] Bellini, A., Fused deposition of Ceramics: A Study of Material Behavior, Fabrication Process and Equipment Design, PhD Thesis, Drexel University, Philadelphia, PA, 2002.